Developmental Cell, Volume *24*

Supplemental Information

Wnt-Dependent Epithelial Transitions Drive Pharyngeal Pouch Formation

Chong Pyo Choe, Andres Collazo, Le A. Trinh, Luyuan Pan, Cecilia B. Moens, and J. Gage Crump

INVENTORY OF SUPPLEMENTAL INFORMATION

SUPPLEMENTAL FIGURES

SUPPLEMENTAL EXPERIMENTAL PROCEDURES

SUPPLEMENTAL REFERENCES

SUPPLEMENTAL FIGURES

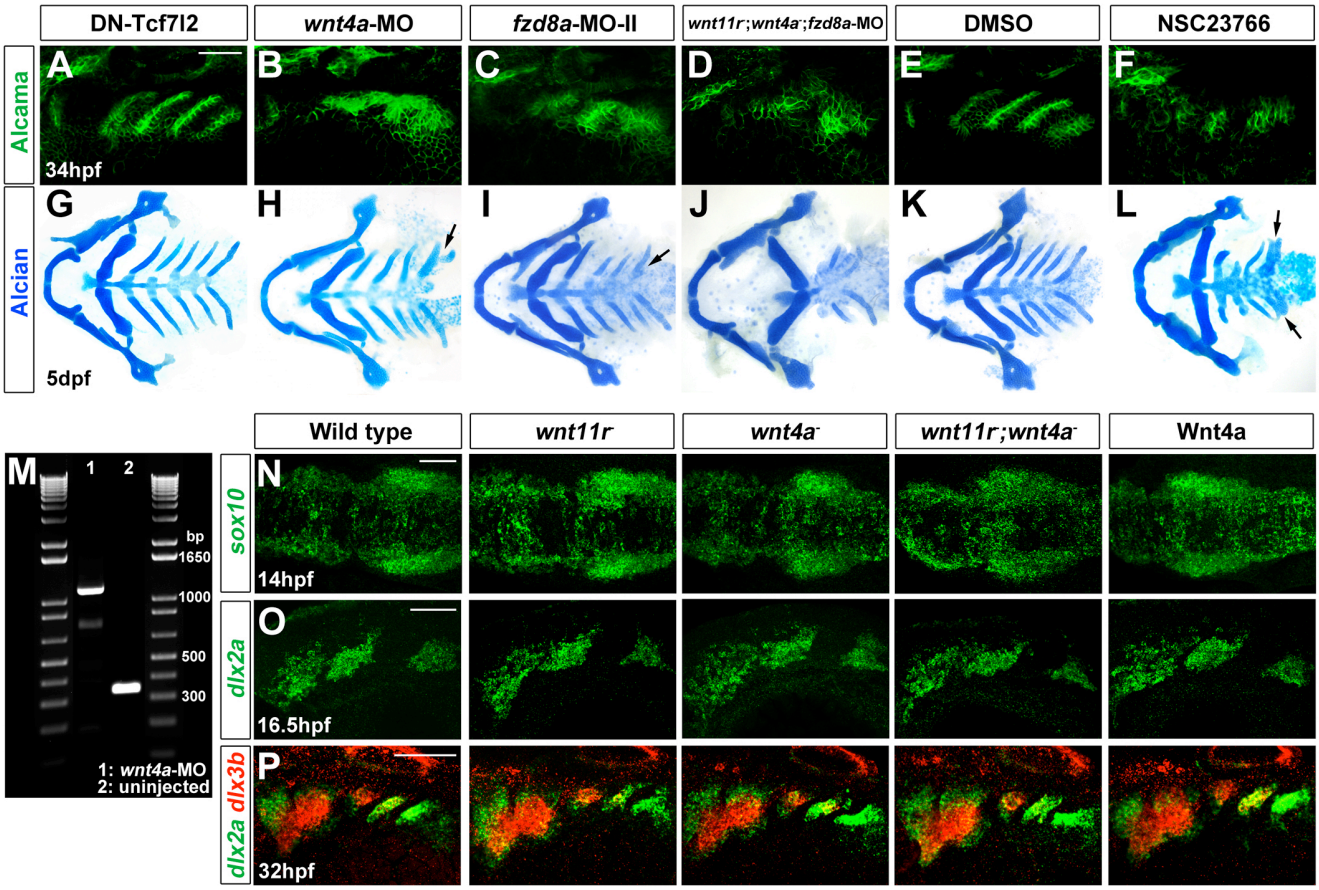

Figure S1, Wnt signaling in pouch, CB cartilage, and neural crest development, related to Figure 3.

(A-L) Alcama immunohistochemistry (A-F) and Alcian Blue staining (G-L) show no pouch or CB cartilage defects upon PE-specific inhibition of nuclear-β-catenin signaling in *nkx2.3*:Gal4VP16; UAS:DN-Tcf7l2 embryos (A and G) or in control embryos incubated in 6% DMSO from 18-26 hpf (E and K). In contrast, severe pouch and CB defects were observed in *wnt4a*-MO (B and H), *fzd8a*-MO-II (C and I), and *fzd8a*-MO-injected *wnt11r*; *wnt4a* double mutants (D and J), as well as embryos incubated in 300 μM of the Rac inhibitor NSC23766 from 18-26 hpf (F and L). Arrows indicate fused or malformed CBs.

(M) In uninjected control embryos, normal splicing of intron 2 of the *wnt4a* gene generates a 333 bp band after PCR amplification. In contrast, one-cell-stage injection of *wnt4a*-MO at 300 μM results in a failure to splice out intron 2, thus resulting in a 1137 bp band (333 bp of exon2/3 and 804 bp of second intron).

(N-P) Fluorescent in situs show normal expression of *sox10* at 14 hpf, *dlx2a* at 16.5 hpf, and *dlx2a* (green) and *dlx3b* (red) at 32 hpf in wild types, mutants, and Wnt4a-misexpression embryos. Wnt4a transgenic embryos (capitalized) were doubly positive for *nkx2.3*:Gal4VP16. The *sox10* in situ shows a dorsal view of early cranial neural crest, and the *dlx2a* and *dlx2a/dlx3b* in situs show lateral views of the developing pharyngeal arches. Anterior is to the left in all images. Scale bars = 40 μM.

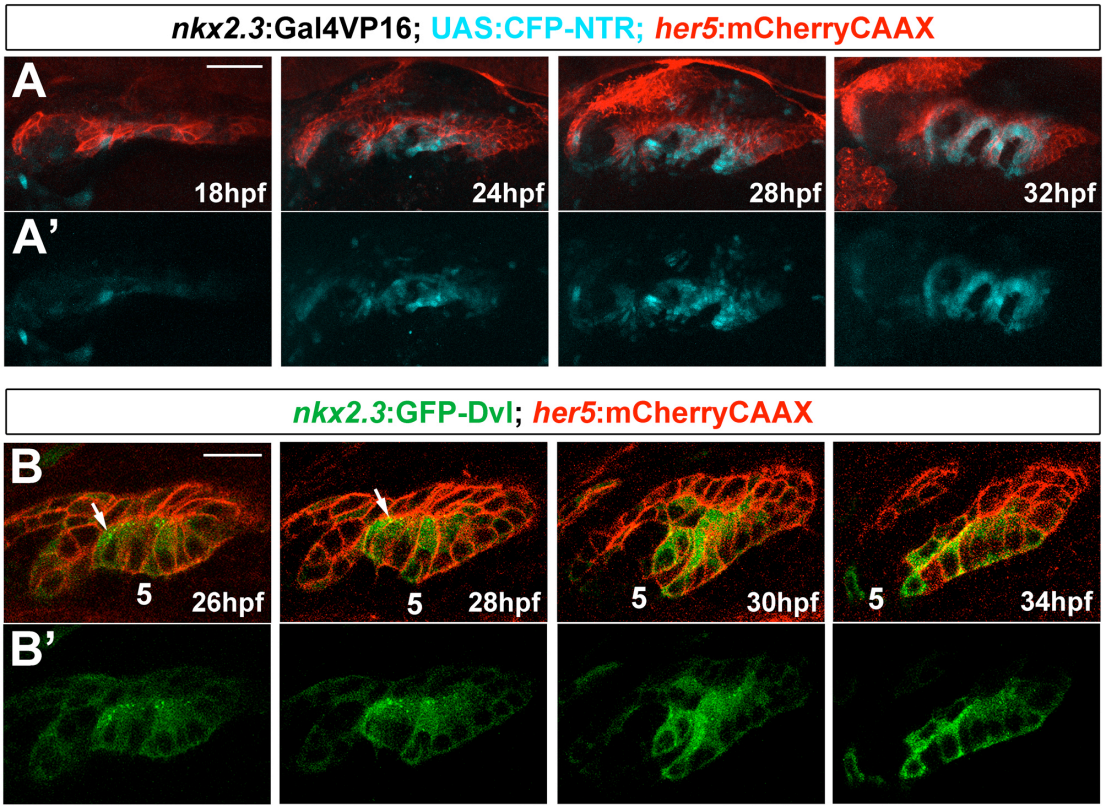

Figure S2, Specificity of *nkx2.3*:Gal4VP16 and GFP-Dvl localization in pouches, related to Figure 3.

(A) Time-course of CFP-NTR expression in *nkx2.3*:Gal4VP16; UAS:CFP-NTR; *her5*:mCherryCAAX transgenic embryos. *nkx2.3*:Gal4VP16-dependent CFP-NTR expression (blue) co-localizes with *her5*:mCherryCAAX-positive pouch-forming endoderm (red) starting at 18 hpf, with expression becoming stronger as pouch development progresses. Views are dorsal-lateral with anterior to the left. Scale bar = 40 μM.

(B) Still images from a time-lapse confocal recording of fifth pouch development in *nkx2.3*:GFP-Dvl; *her5*:mCherryCAAX transgenic embryos (see Movie S5). GFP-Dvl (green) localizes to apical puncta (arrows) during remodeling of the *her5*:mCherryCAAX-positive endoderm (red) to form pouches. Scale bar = 20 μM.

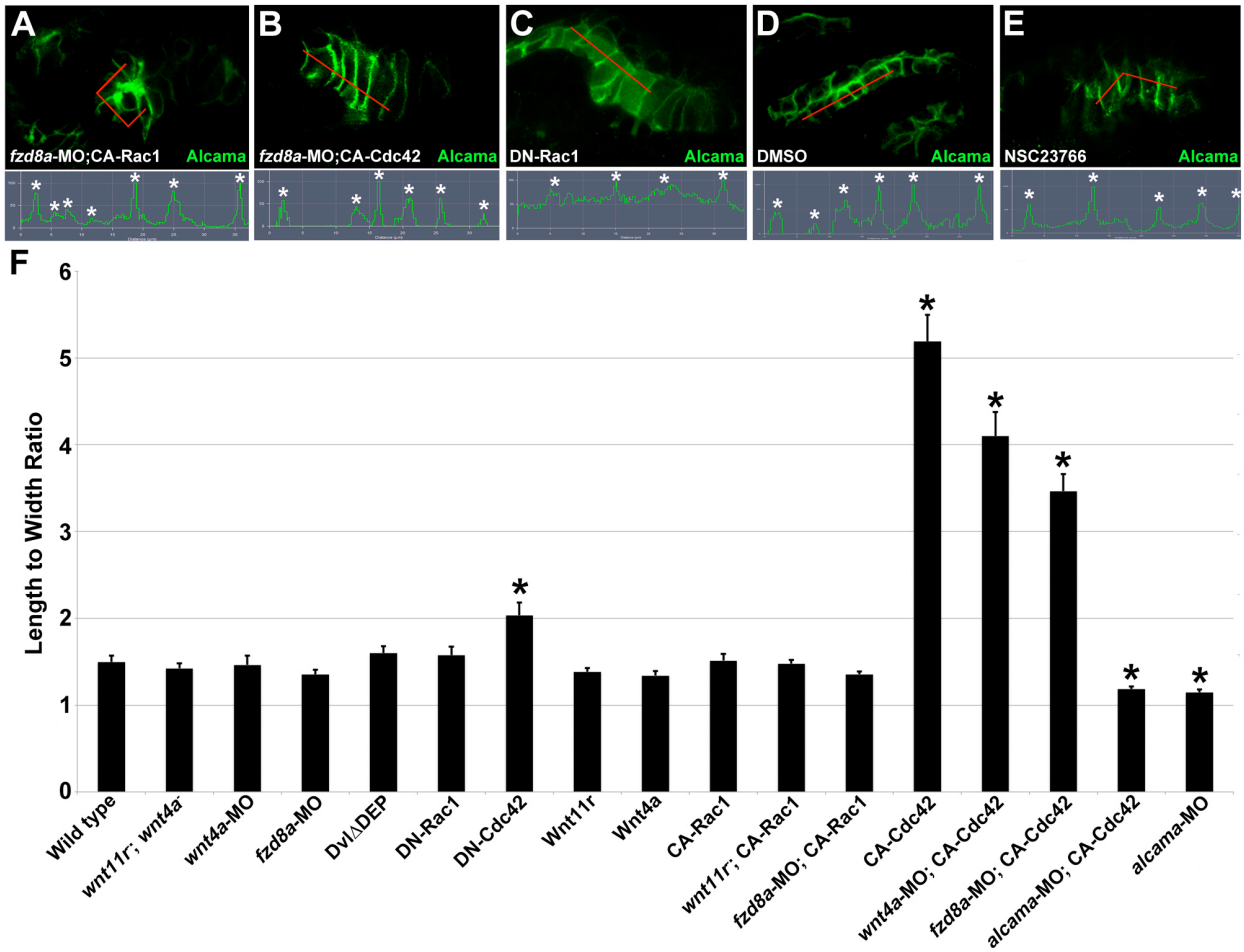

Figure S3, Alcama localization in rescued *fzd8a*-MO and Rac-inhibited embryos and quantification of cell shape, related to Figure 4.

(A-E) Immunohistochemistry shows Alcama localization in 34 hpf pouch-forming endoderm in *fzd8a*-MO-injected *nkx2.3*:Gal4VP16; UAS:CA-Rac1 embryos (A), *fzd8a*-MO-injected *nkx2.3*:Gal4VP16; UAS:CA-Cdc42 embryos (B), *nkx2.3*:Gal4VP16; UAS:DN-Rac1 embryos (C), control embryos incubated in 6% DMSO from 18-26 hpf (D), and embryos incubated in the Rac inhibitor NSC23766 in 6% DMSO from 18-26 hpf (E). The normalized intensity of fluorescent signal is plotted along the 35 μM red lines. Asterisks indicate identifiable cell-cell boundaries. Activated Rac1 resulted in rosette-like structures in 59/81 *fzd8a*-MO-injected embryos, and activated Cdc42 rescued Alcama membrane localization and induced hyper-elongated cell shape in 24/63 *fzd8a*-MO-injected embryos.

(F) Quantification of 34 hpf pouch cell shape in wild type, mutants, *fzd8a*-MO, and embryos doubly transgenic for UAS transgenes (capitalized) and *nkx2.3*:Gal4VP16. The ratios of the longest versus shortest cell axes are plotted. Asterisks indicate significant differences compared to wild type ($p<0.05$ in a student's t-test). Data represent mean ± SEM. Total cells analyzed: Wild type (96), *wnt11r*$^{-}$; *wnt4a*$^{-}$ (100), *fzd8a*-MO (97), *nkx2.3*:Gal4VP16; UAS:DvlΔDEP (100), *nkx2.3*:Gal4VP16; UAS:DN-Rac1 (96), *nkx2.3*:Gal4VP16; UAS:DN-Cdc42 (92), *nkx2.3*:Gal4VP16; UAS:Wnt11r (45), *nkx2.3*:Gal4VP16; UAS:Wnt4a (100), *nkx2.3*:Gal4VP16; UAS:CA-Rac1 (92), *fzd8a*-MO; *nkx2.3*:Gal4VP16; UAS:CA-Rac1 (81), *wnt11r*$^{-}$; *nkx2.3*:Gal4VP16; UAS:CA-Rac1 (48), *nkx2.3*:Gal4VP16; UAS:CA-Cdc42 (88), *wnt4a*-MO; *nkx2.3*:Gal4VP16; UAS:CA-Cdc42 (53), *fzd8a*-MO; *nkx2.3*:Gal4VP16; UAS:CA-Cdc42 (57), *alcama*-MO; *nkx2.3*:Gal4VP16; UAS:CA-Cdc42 (60), and *alcama*-MO (95).

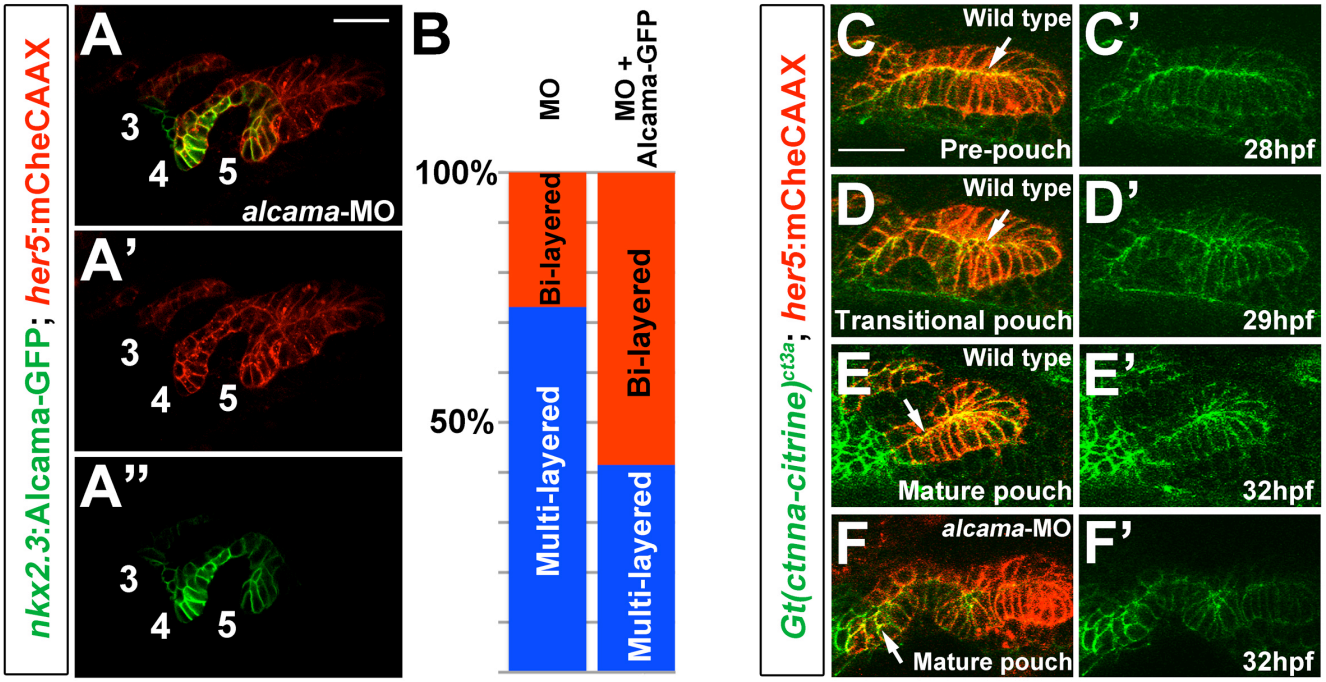

Figure S4, Requirement of Alcama in endoderm and its role in α-catenin localization, related to Figure 5.

(A) Transgenic expression of Alcama-GFP in *nkx2.3*:Alcama-GFP; *her5*:mCherryCAAX embryos partially restores bilayered pouch morphology to *alcama*-MO-injected embryos. Alcama-GFP (green) localizes to apical and lateral membranes of pouches labeled with *her5*:mCherryCAAX (red). Pouches 3-5 are numbered. Scale bar = 20 μM.

(B) Quantification of rescue of *alcama*-MO pouch defects by Alcama-GFP transgenic expression. Pouches 4 and 5 were used for the analysis. n=119 for *alcama*-MO + Alcama-GFP, and n=118 for *alcama*-MO alone. p-value = 0.000001.

(C-E) Still images from a time-lapse confocal recording of fifth pouch development in a *Gt(ctnna-citrine)*^{ct3a}; *her5*:mCherryCAAX embryo (See Movie S7). In the pre-pouch endoderm, α-catenin-citrine (green) is enriched along apical membranes (arrows) of the *her5*:mCherryCAAX-labeled endodermal bilayer (red). During pouch initiation, α-catenin-

citrine becomes less organized in the multi-layered transitional epithelium. As pouches mature, α-catenin-citrine becomes organized again along apical membranes in the bilayer.

(F) At a stage when wild-type pouches would have matured into bilayers, α-catenin-citrine remains disorganized in the *alcama*-MO multilayered pouches (arrow).

SUPPLEMENTAL EXPERIMENTAL PROCEDURES

Transgenic zebrafish lines

Gt(ctnna-citrine)^{ct3a} was isolated in a FlipTrap screen as described (Trinh et al., 2011). Upstream regulatory regions of the *hairy-related 5* (*her5*), *NK2 transcription factor related 3* (*nkx2.3*), or *NK2 transcription factor related 5* (*nkx2.5*) genes were amplified from multi-stage zebrafish genomic DNA by using the Expand Long Range dNTPack (Roche Applied Science). The PCR products (0.7 kb from *her5*; 5.5 kb from *nkx2.3*; and 5.9 kb from *nkx2.5*) were cloned into the pDONR P4-P1R vector to generate p5E-*her5*, p5E-*nkx2.5*, and p5E-*nkx2.3*. p5E-*her5* was combined with pME-mCherryCAAX, p3E-polyA, and pDestTol2pA2 to generate the *her5*:mCherryCAAX:pA construct. A total of five independent transgenic lines of *Tg(her5:mCherryCAAX)* were isolated based on mCherryCAAX expression in pharyngeal endoderm (PE), and *Tg(her5:mCherryCAAX)*^{el72} showed the brightest mCherryCAAX expression and was used in this study. p5E-*nkx2.5* was combined with pME-GFP, p3E-polyA, and pDestTol2pA2 to generate the *nkx2.5*:GFP:pA construct. A total of eight independent lines of *Tg(nkx2.5:GFP)* were produced based on GFP expression in the mesoderm, and *Tg(nkx2.5:GFP)*^{el83} showed the brightest GFP expression and was used in this study. p5E-*nkx2.3* was combined with pME-Gal4VP16, p3E-polyA, and pDestTol2CG2 to generate the *nkx2.3*:Gal4VP16:pA construct. p5E-*nkx2.5* was combined with pME-Gal4VP16, p3E-polyA,

and pDestTol2CG2 to generate the *nkx2.5*:Gal4VP16:pA construct. Five independent lines of *Tg(nkx2.5:Gal4VP16)* and seven of *Tg(nkx2.3:Gal4VP16)* were tested with *Tg(UAS:CFP-NTR)*^{el53}, and the strongest alleles - *Tg(nkx2.5:Gal4VP16)*^{el74} and *Tg(nkx2.3:Gal4VP16)*^{el93} – were used in this study.

A deletion or point mutation was induced by fusion PCR to generate DvlΔDEP, Rac1N17, Rac1V12, Cdc42N17, or Cdc42V12. To generate DvlΔDEP, two cDNA fragments of *dishevelled2* (*dvl2*) were amplified separately by PCR (Phusion, NEB) from zebrafish multi-stage cDNA using primers that produce overlapping ends. A second PCR using 'nested' primers fused the fragments into a single fragment with deletion of the DEP domain. The single fragment was cloned into the middle entry pDONR221 vector to generate pME-DvlΔDEP. To induce Rac1 or Cdc42 point mutations, two cDNA fragments of *ras-related C3 botulinum toxin substrate 1* (*rac1*) or *cell division cycle 42* (*cdc42*) were amplified first by PCR using primers that produce overlapping ends and include the desired point mutation. A second PCR using 'nested' primers fused the fragments into a single fragment, with single fragments cloned into the middle entry pDONR221 vector to generate pME-Rac1N17, pME-Rac1V12, pME-Cdc42N17, or pME-Cdc42V12. Each of the middle entry vectors was combined with p5E-UAS, p3E-polyA, and pDestTol2AB to generate UAS:DvlΔDEP:pA, UAS:Rac1N17:pA, UAS:Rac1V12:pA, UAS:Cdc42N17:pA, and UAS:Cdc42V12:pA constructs. Five each of *Tg(UAS:DvlΔDEP:pA)*, *Tg(UAS:Rac1N17:pA)*, *Tg(UAS:Cdc42N17:pA)*, and *Tg(UAS:Cdc42V12:pA)*; and three *Tg(UAS:Rac1V12:pA)* independent transgenic lines were isolated based on α*-crystallin*:Cerulean which produces blue fluorescence in the lens. For phenotypic analyses, UAS transgenic lines were crossed with *Tg(nkx2.3:Gal4VP16)*^{el93} and animals carrying both *cmcl2*:GFP and α*-crystallin*:Cerulean were analyzed, with *cmcl2*:GFP-only embryos serving as internal controls. Each allele within

a UAS line showed similar phenotypes in both pouch and CB development. We used *Tg(UAS:DvlΔDEP)*^{el190}, *Tg(UAS:RacN17)*^{el262}, *Tg(UAS:RacV12)*^{el320}, *Tg(UAS:Cdc42N17)*^{el268}, and *Tg(UAS:Cdc42V12)*^{el322} for further analysis as they displayed the highest penetrance and severity of pouch and CB defects in conjunction with *Tg(nkx2.3:Gal4VP16)*^{el93}.

To generate the *nkx2.3*:GFP-Dvl:pA construct, the coding sequence of Dvl2 was amplified from multi-stage zebrafish cDNA by PCR and then cloned into the 3' entry pDONR P2R-P3 vector to generate p3E-Dvl. The p3E-Dvl was combined with p5E-*nkx2.3*, pME-GFP, and pDestTol2CG2. A total of three independent lines of *Tg(nkx2.3:GFP-Dvl)* were established based on GFP expression in PE, and *Tg(nkx2.3:GFP-Dvl)*^{el303} showed the brightest GFP expression and was used in this study. The coding sequence of Alcama without the stop codon was amplified from multi-stage zebrafish cDNA by PCR and cloned into the middle entry pDONR221 vector to generate pME-Alcama. pME-Alcama was combined with p5E-*nkx2.3*, p3E-GFP, and pDestTol2CG2. A total of four independent lines of *Tg(nkx2.3:Alcama-GFP)* were isolated based on GFP expression in PE, and *Tg(nkx2.3:Alcama-GFP)*^{el304} showed the brightest GFP expression and was used in this study. To generate the UAS:Wnt11r construct, the full length sequence of Wnt11r was amplified from multi-stage zebrafish cDNA by PCR and cloned into pDONR221 to generate pME-Wnt11r. pME-Wnt11r was combined with p5E-UAS, p3E-pA, and pDestTol2AB. Three independent lines of *Tg(UAS:Wnt11r)* were isolated based on α-*crystallin*:Cerulean. The three lines showed a similar range of pouch and CB defects in conjunction with *Tg(nkx2.3:Gal4VP16)*^{el93} and *Tg(UAS:Wnt11r)*^{el421} was used in this study. To generate the UAS:Wnt4a construct, the coding sequence of Wnt4a was amplified from multi-stage zebrafish cDNA by PCR and cloned into pDONR221 to generate pME-Wnt4a. pME-Wnt4a was combined with p5E-UAS, p3E-pA, and pDestTol2CG2. Two independent lines of

Tg(UAS:Wnt4a) were isolated based on *cmlc2*:GFP. The two lines showed a similar range of pouch and CB defects in conjunction with *Tg(nkx2.3:Gal4VP16)*^{el93} and *Tg(UAS:Wnt4a)*^{el48} was used in this study. To generate the UAS:CFP-NTR construct, the coding sequence of CFP-NTR was amplified from the tol2_CFP_NTR plasmid (Curado et al., 2008) by PCR and cloned into pDONR221 to generate pME-CFP-NTR. pME-CFP-NTR was combined with p5E-UAS, p3E-pA, and pDestTol2CG2. Four independent lines of *Tg(UAS:CFP-NTR:pA)* were isolated based on *cmlc2*:GFP, and *Tg(UAS:CFP-NTR:pA)*^{el53} was used in this study.

The following primers were used to generate constructs:

her5-B4F: 5'-GGGGACAACTTTGTATAGAAAAGTTGACTGCAGAAACACCATTGGA-3'

her5-B1R: 5'- GGGGACTGCTTTTTTGTACAAACTTGGCGGCCGCCATGCAGCTCTA-3'

nkx2.5-B4F: 5'-GGGGACAACTTTGTATAGAAAAGTTGCCCAAGCCCACTTACCAATA-3'

nkx2.5-B1R: 5'-GGGGACTGCTTTTTTGTACAAACTTGGGATAATCCGGTTGGGATTT-3'

nkx2.3-B4F: 5'-GGGGACAACTTTGTATAGAAAAGTTGAGGGCATAGCTAATGGGGA-3'

nkx2.3-B1R: 5'-GGGGACTGCTTTTTTGTACAAACTTGGGCGCTGTTGGATTACATCT-3'

Dvl-B1F: 5'-GGGGACAAGTTTGTACAAAAAAGCAGGCTAGCGTTAGCAGGATAAGTTAG-3'

Dvl-MR: 5'-GATTGTGCTGCTAGGCTCAATACG-3'

Dvl-MF: 5'-CGTATTGAGCCTAGCAGCACAATC-3'

Dvl-B2R: 5'-GGGGACCACTTTGTACAAGAAAGCTGGGTGTTATTTAGAAGGCCAGACC-3'

Rac1-B1F: 5'-GGGGACAAGTTTGTACAAAAAAGCAGGCTTGGCTGTTTGTTTAACTGG-3'

Rac1(N17)-MR: 5'-AGAAGGCAATTTTTTCCC-3'

Rac1(N17)-MF: 5'-GGGAAAAAATTGCCTTCT-3'

Rac1(V12)-MR: 5'-ACAGCCACGTCCCC-3'

Rac1(V12)-MF: 5'-GGGGACGTGGCTGT-3'

Rac1-B2R: 5'-GGGGACCACTTTGTACAAGAAAGCTGGGTTGGAGACAGTAAAAGCATGA-3'

Cdc42-B1F: 5’-GGGGACAAGTTTGTACAAAAAAGCAGGCTCTTGAATGAGAGCAGTGGA-3’

Cdc42(N17)-MR: 5’-TTAATAGACAGTTTTTACCCACT-3’

Cdc42(N17)-MF: 5’-AGTGGGTAAAAACTGTCTATTAA-3’

Cdc42(V12)-MR: 5’- CCACTGCAACATCACCA-3’

Cdc42(V12)-MF: 5’-TGGTGATGtTGCAGTGG-3’

Cdc42-B2R: 5’-GGGGACCACTTTGTACAAGAAAGCTGGGTCAGAGCATTTGGTGTTTCA-3’

Dvl-B2F: 5’-GGGGACAGCTTTCTTGTACAAAGTGGTTATGGCGGAGACCAAGA-3’

Dvl-B3R: 5’-GGGGACAACTTTGTATAATAAAGTTGTTACATCACATCCACAAAAAAC-3’

Alcam-B1F: 5’-GGGGACAAGTTTGTACAAAAAAGCAGGCTATGCATTCGGTTATCTGC-3’

Alcam-B2R: 5’-
GGGGACCACTTTGTACAAGAAAGCTGGGTGACATCTGCTTTATGATTGTTC-3’

Wnt11r-B1F: 5’- GGGGACAAGTTTGTACAAAAAAGCAGGCTGAGCAGCACCACAAACC-3’

Wnt11r-B2R: 5’- GGGGACCACTTTGTACAAGAAAGCTGGGTTTACGCTCCACACCCAG-3’

Wnt4a-B1F: 5’-GGGGACAAGTTTGTACAAAAAAGCAGGCTATGCCAACAGTCTCCTC-3’

Wnt4a-B2R: 5’-GGGGACCACTTTGTACAAGAAAGCTGGGTTTATTCTCGGCAGGTGTG-3’

CFP-NTR-B1F: 5’-
GGGGACAAGTTTGTACAAAAAAGCAGGCTATGGTGAGCAAGGGCGAGGA-3’

CFP-NTR-B2R: 5’-
GGGGACCACTTTGTACAAGAAAGCTGGGTATGGTGAGCAAGGGCGAGGA-3’

Whole-mount in situ hybridization

Published probes include *sox10* and *dlx2a* (Das and Crump, 2012) and *dlx3b* (Zuniga et al., 2011). PCR amplification generated DNA fragments from the *nkx2.5* (668 bp), *wnt11r* (612 bp), *wnt4a* (604 bp), or *fzd8a* (634 bp) genes. PCR products were cloned into pGEM®-T

Easy Vector Systems (Promega). T7 or SP6 RNA polymerase was used to synthesize riboprobes from linearized plasmids for whole-mount in situ hybridization. The following primers were used:

nkx2.5-r-F: 5'-CATCCGGATCCTCTCTCT-3'

nkx2.5-r-R: 5'-GCTGTTGGACTGTGAAGG-3'

wnt11r-r-F: 5'-AGACCTGGAACGAGGAAC-3'

wnt11r-r-R: 5'-CCGCTGGATGTCTTATTG-3'

wnt4a-r-F: 5'-GGGAAAGTGGTCACACAA-3'

wnt4a-r-R: 5'-GTCTTGTTGCAGAATCGG-3'

fzd8a-r-F: 5'-GCTACCTGTTGGGGATTT-3'

fzd8a-r-R: 5'-TTAACGCGGTTGTAGAGC-3'

Confirmation of the efficiency of *wnt4a*-MO

The efficiency of *wnt4a*-MO was analyzed by RT-PCR using the following primers spanning the second intron of the *wnt4a* gene.

wnt4a-E2F: 5'- GTGGGGAGCATCTCTGAT-3'

wnt4a-E3R: 5'- TCCGTGAACATTACGGTC-3'

SUPPLEMENTAL REFERENCES

Das, A., and Crump, J.G. (2012). Bmps and id2a act upstream of Twist1 to restrict ectomesenchyme potential of the cranial neural crest. PLoS Genet *8*, e1002710.

Trinh, L.A., Hochgreb, T., Graham, M., Wu, D., Ruf-Zamojski, F., Jayasena, C.S., Saxena, A., Hawk, R., Gonzalez-Serricchio, A., Dixson, A.*, et al.* (2011). A versatile gene trap to visualize and interrogate the function of the vertebrate proteome. Genes Dev *25*, 2306-2320.